Primary Steps in the Hydrolyses of Two Heterometallic Alkoxides. Characterization of $[LiTiO(O^iPr)_3]_4$ and $BaZr_4(OH)(O^iPr)_{17}$

Roger Kuhlman,[†] Brian A. Vaartstra,[‡] William E. Streib,[†] John C. Huffman,[†] and Kenneth G. Caulton*,[†]

Department of Chemistry and Molecular Structure Center, Indiana University, Bloomington, Indiana 47405, and Advanced Technology Materials, Inc., Danbury, Connecticut 06810

Received November 25, 1992

Partial hydrolysis of $[LiTi(O^iPr)_5]_2$ yields a tetrameric oxo-alkoxide, $[LiTiO(O^iPr)_3]_4$. The compound has been characterized in solution by ^1H and ^{13}C NMR spectroscopy and in the solid state by X-ray crystallography. The molecule crystallizes in the space group $C2/c$ with a = 18.460(3) Å, b = 17.904(3) Å, c = 15.832(2) Å, β = 90.11(0)°, and Z = 4. Titanium and oxo atoms are located in a middle layer with Li atoms in layers above and below, supported by alkoxide bridges. The similarity to ferroelectric titanates is evident in the coordination sphere of Ti in $[LiTiO(O^iPr)_3]_4$. Addition of 1 equiv of water to $BaZr_4(O^iPr)_{18}$ in THF yields the hydroxide $BaZr_4(OH)(O^iPr)_{17}$ in a simple acid/base ligand exchange reaction. Characterization by X-ray diffraction shows that the molecule crystallizes in the $C2/c$ space group, with dimensions a = 58.735(12) Å, b = 12.555(13) Å, c = 19.321(4) Å, and β = 94.17(1)° (Z = 8). Variable-temperature ^1H and ^{13}C NMR data are also reported, revealing ligand site exchange local to $BaZr_2$ triangles. The hydroxide ligand adopts a μ_3-site, bridging the barium and two zirconium atoms. In both cases, the metal stoichiometry has been retained in the final product.

Introduction

Ferroelectric ceramics such as lead titanate, lead zirconate titanate (PZT), barium titanate, and barium strontium titanate are highly acclaimed for their applications in electrooptic, piezoelectric, and pyroelectric devices. The conventional methods for growth of ferroelectric thin films have been sputtering techniques, which suffer the disadvantages of low rates of deposition, surface inhomogeneity, and, most importantly, poor stoichiometric control from target to substrate.[1] Alternative approaches include spin-on techniques such as metalorganic deposition (MOD) and sol–gel processing. These are advantageous over sputtering because molecular precursors are homogeneously mixed in the appropriate ratio in solution.

The structural and electronic relationship between metal oxides and metal alkoxides has been pointed out as a prime reason for using alkoxide precursors in the preparation of oxide ceramics.[2-4] In addition, alkoxides can generally be highly purified by distillation or sublimation and are usually stable enough to be stored indefinitely.[4] The alkoxide precursor can be decomposed at relatively low temperature with concomitant loss of volatile organic byproducts which are not incorporated into the oxide film. If metal alkoxides are indeed good precursors for metal oxides it is reasonable to extend this argument to hetero*bi*metallic alkoxides as potential precursors for bimetallic oxides.[5] A bimetallic precursor has the potential to control stoichiometry at the molecular level and thus make this critical parameter less sensitive to processing conditions.

If single-source materials are to become an advantage for stoichiometric control of resultant oxide materials, it is reasonable to require that the conversion process maintain this advantage throughout. In the case of sol–gel processing, hydrolysis steps proceed via intermediates which would ideally retain the original metal stoichiometry. One concern is that hydrolysis of a heterometallic alkoxide containing metals with very different metal hydroxide/oxide solubilities might undergo metal "segregation" with rapid precipitation of only one of the hydrous metal oxides. If this is not to occur, it must be true that the intermediate $M_aM'_bO_m(OR)_n$ (and the successor polymeric sol network) contains a sufficiently good sequestering agent (i.e., ligand) for the least-soluble oxide, such that the thermodynamics of precipitation of monometal oxide are overcome.

We have been investigating the nature of intermediates in the hydrolysis of mixed-metal alkoxides in order to establish the viability of molecular stoichiometric control for the deposition of oxide ceramics. Herein we present our investigation of the hydrolysis products from two different bimetallic alkoxides. This approach of studying the initial stages of hydrolysis has been pioneered for homometallic (titanium) alkoxides by the group of Klemperer.[6]

Experimental Section

All reactions and manipulations were performed under an atmosphere of dry nitrogen or in vacuo, using standard Schlenk and glovebox techniques, unless otherwise specified. Solvents used were initially dried, distilled, and stored under nitrogen over molecular sieves. The starting materials, $BaZr_4(O^iPr)_{18}$[7] and $[LiTi(O^iPr)_5]_2$,[8] were synthesized according to the literature. ^1H and $^{13}C\{^1H\}$ NMR spectra were recorded on either a Varian XL-300 or a Bruker AM-500 spectrometer and chemical shifts referenced to residual solvent peaks. Infrared spectra were recorded on a Nicolet 510P FTIR spectrometer.

Synthesis of $[LiTiO(O^iPr)_3]_4$. The alkoxide dimer $[LiTi(O^iPr)_5]_2$ (0.800 g, 1.13 mmol) was dissolved in THF (15 mL) and treated with a THF (20 mL) solution of H_2O (40.6 μL, 2.25 mmol). The solution was stirred for 5 min, and then the solvent was removed in vacuo, leaving a white solid. The solid was dissolved in a minimum amount of pentane, and large, colorless, square prismatic crystals of $[LiTiO(O^iPr)_3]_4$ (0.300 g, 0.302 mmol, 53.5% isolated yield) were grown by slow cooling to −15 °C.[9] ^1H NMR (toluene-d_8): δ 4.86 (sept, 2H), 4.84 (sept. 4H), 4.81 (sept, 2H), 4.73 (sept, 4H), 1.53 (d, 12H), 1.42 (d, 12H), 1.41 (d, 12H),

[†] Indiana University.
[‡] Advanced Technology Materials.

(1) Nakagawa, T.; Yamaguchi, J.; Okuyama, M.; Hamakawa, Y. *Jpn. J. Appl. Phys.* **1982**, *21*, L665.
(2) Chisholm, M. H. *Inorganic Chemistry Toward the 21st Century*; American Chemical Society: Washington, DC, 1983; Chapter 16, p 243.
(3) Hubert-Pfalzgraf, L. G. *New J. Chem.* **1987**, *11*, 663.
(4) Bradley, D. C. *Chem. Rev.* **1989**, *89*, 1317.
(5) Caulton, K. G.; Hubert-Pfalzgraf, L. G. *Chem. Rev.* **1990**, *90*, 969–995.
(6) Day, V. W.; Eberspacher, T. A.; Klemperer, W. G.; Park, C. W.; Rosenberg, F. S. *J. Am. Chem. Soc.* **1991**, *113*, 8190.
(7) Vaartstra, B. A.; Huffman, J. C.; Streib, W. E.; Caulton, K. G. *Inorg. Chem.* **1991**, *30*, 3068.
(8) Hampden-Smith, M. J.; Williams, D. S.; Rheingold, A. L. *Inorg. Chem.* **1990**, *29*, 4076.

0020-1669/93/1332-1272$04.00/0

Table I. Crystallographic Data

$[LiTiO(O^iPr)_3]_4$			
chemical formula	$C_{36}H_{84}Li_4O_{16}Ti_4$	space group	$C2/c$
a, Å	18.460(3)	T, °C	−176
b, Å	17.904(3)	λ, Å	0.710 69
c, Å	15.832(2)	ρ_{calcd}, g cm^{-3}	1.260
β, deg	90.11(0)	μ(MoKα), cm^{-1}	6.37
V, Å^3	5232.80	R	0.0366
Z	4	R_w	0.0394
fw	992.41		

$BaZr_4(OH)(O^iPr)_{17}$			
chemical formula	$C_{51}H120BaO_{18}Zr_4$	space group	$C2/c$
a, Å	58.735(12)	T, °C	−150
b, Å	12.555(3)	λ, Å	0.710 69
c, Å	19.321(4)	ρ_{calcd}, g cm^{-3}	1.425
β, deg	94.17(1)	μ(MoKα), cm^{-1}	11.59
V, Å^3	14 209.50	R	0.0619
Z	8	R_w	0.0606
fw	1523.72		

1.36 (d, 12H), 1.28 (d, 12H), 1.25 (d, 12H). $^{13}C\{^1H\}$ NMR (toluene-d_8): δ 75.99, 75.65, 73.24, 69.51, 28.76, 28.15, 27.72, 27.08, 26.67, 26.31 (singlets). IR (KBr): 1162 (vs), 1129 (vs), 1011 (s), 980 (m), 968 (vs), 835 (w), 715 (s), 653 (m), 592 (vs) cm^{-1}.

Synthesis of $BaZr_4(OH)(O^iPr)_{17}$. To a solution of $BaZr_4(O^iPr)_{18}$ (0.400 mg, 0.26 mmol) in THF (20 mL) was added 1 equiv of H_2O (4.6 μL, 0.26 mmol) in THF (20 mL) dropwise with constant stirring. After the addition, the solution was stirred for 5 min, and then the volume was reduced to about 15 mL in vacuo. After 1 week at −15 °C, colorless prisms of $BaZr_4(OH)(O^iPr)_{17}$ had grown; these were suitable for X-ray diffraction (0.140 g, 0.098 mmol, 38% yield). ^1H NMR (toluene-d_8, 86 °C): δ 1.47 (d, 54H), 1.42 (d, 48H). $^{13}C\{^1H\}$ NMR (toluene-d_8, −32 °C): δ 71.37, 71.17, 70.78, 70.14, 69.74, 69.16, 68.46, 68.33, 68.18, 67.73, 28.18 (br), 28.11 (br), 27.72 (br), 27.26 (br), 27.16 (br), 27.05 (br), 26.94 (br), 26.83 (br) (singlets). IR (KBr): 1174 (vs), 1131 (vs), 1022 (vs), 1007 (vs), 966 (s), 954 (s), 845 (w), 829 (w), 819 (w) cm^{-1}.

X-ray Diffraction. General Information. A crystal was transferred to a glovebag and was affixed to the end of glass fiber using silicone grease. The crystal was then transferred to the goniostat where it was cooled for characterization (Table I) and data collection ($6° < 2\theta < 45°$).[10] A systematic search of a limited hemisphere of reciprocal space located a set of diffraction maxima with symmetry and systematic absences corresponding to one of the monoclinic space groups Cc or $C2/c$. Subsequent solution and refinement confirmed the centrosymmetric choice, $C2/c$. Data were collected using a standard θ–2θ continuous scan with fixed background counts at each extreme of the scan.

X-ray Structure Determination of $[LiTiO(O^iPr)_3]_4$. After correction for Lorentz and polarization effects, equivalent data were averaged (R = 0.043) to yield a set of unique intensities and σ's. The structure was solved by a combination of direct methods (SHELX76) and Fourier techniques. All atoms (including hydrogen atoms) were located and refined in the full-matrix least-squares refinement. Hydrogen atoms were assigned isotropic thermal parameters, and all other atoms, anisotropic parameters. A final difference Fourier was featureless, the largest peak being 0.36 e/Å^3. Results of the structure determination are shown in Tables II and III and Figure 1.

X-ray Structure Determination of $BaZr_4(OH)(O^iPr)_{17}$. Data processing gave a residual of 0.067 for the averaging of 3242 unique intensities which had been observed more than once. Four standards measured every 300 data showed no significant trends. No correction was made for absorption. The structure was solved using a combination of direct methods (SHELXS-86) and Fourier techniques. The positions of the Ba and Zr atoms were obtained from subsequent iterations of least-squares refinement and difference Fourier calculation. The hydrogens bonded to the carbon atoms were included in fixed calculated positions with thermal parameters fixed at 1 plus the isotropic thermal parameter of the atom to which they were bonded. The hydrogen on the OH ligand was not observed in the difference maps and was not included in the refinement. In the final cycles of refinement, all of the non-hydrogen atoms were varied with anisotropic thermal parameters. The largest peaks in the final difference map were Ba and Zr residuals of 0.84–1.34 e/Å^3 and a peak of 1.13 e/Å^3 in the vicinity of the C(48)–C(50) isopropyl group. This later peak, together with somewhat abnormal bond distances and angles for this group, suggested a small amount of disorder there. Because of the small electron density of the residual peak, no attempt was made to resolve the disorder. The largest hole was −1.17 e/Å^3. The results are shown in Tables IV and V and Figure 2.

(9) The actual yield was much higher, based on ^1H NMR of the crude product. Crystals actually used in X-ray diffraction were grown by diffusion of moist air through a septum into a pentane solution of $\{LiTi(O^iPr)_5\}_2$. The bulk crystalline product of synthesis was shown to be identical by cell constant determination.

(10) For general crystallographic methods and programs employed, see Huffman, J. C.; Lewis, L. N.; Caulton, K. G. *Inorg. Chem.* **1980**, *19*, 2755.

Results

Synthesis of $[LiTiO(O^iPr)_3]_4$. The compound of empirical formula $LiTi(O^iPr)_5$ is in fact a dimer (I) of C_{2h} symmetry with

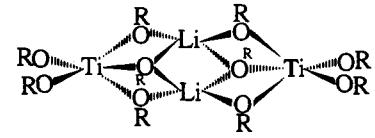

I

two equivalent five-coordinate Ti(IV) centers.[8] Each titanium has a (somewhat distorted) trigonal bipyramidal coordination sphere, and each lithium has a geometry severely distorted (i.e., flattened along a C_2 axis) from tetrahedral. Hydrolysis of this molecule proceeds in high yield to give a crystalline product whose infrared spectrum is devoid of O–H stretching bands in the 3100–3300-cm^{-1} region. Reaction of $[LiTi(O^iPr)_5]_2$ with 3.0 equiv of H_2O (1.5 H_2O/Li) yields $[LiTiO(O^iPr)_3]_4$ as the only ^1H NMR observable species in solution and a colorless precipitate which is insoluble in benzene, acetone, or $CHCl_3$. We believe, therefore, that $[LiTiO(O^iPr)_3]_4$ is the only soluble intermediate in the hydrolysis reaction and that solution characterization of any further hydrolysis step is frustrated by insolubility.

Solid-State Structure of $[LiTiO(O^iPr)_3]_4$. The structure (Figure 1) of the central portion was shown by X-ray diffraction to be a double (face-shared) cube of formula $Li_4Ti_2O_2(O^iPr)_{10}^{2-}$, with two *exo*-$TiO(O^iPr)^+$ groups. The titaniums within the double cube are six-coordinate, while those outside are five-coordinate. The molecule can also be seen to be layered, with two Li_2O_2 planes (where O represents the oxygen of a bridging ^{i}PrO ligand) sandwiching a Ti_4O_4 layer (where O represents an oxo ligand). The middle layer has a Ti(1)–O(3)–Ti(2)′ angle of 163.44(13)°, and an O(3)–Ti(1)–O(4)′ angle of 155.01(10)°, so the layer is stepped: each *individual* Ti_2O_2 rectangle (Ti(1)–O(3)–Ti(2)–O(4), Ti(1)–O(3)–Ti(1)′–O(3)′, and Ti(1)′–O(3)′–Ti(2)′–O(4)′) is planar, but the entire Ti_4O_4 *layer* is not. Therefore, the molecule has neither a crystallographic proper axis of rotation nor a mirror plane, but possesses crystallographic C_i symmetry. The layers are held together by a bonding interaction of the Li atoms with the μ_5-oxygens of the "internal" $Ti(1)_2O(3)_2$ plane, and of the internal Ti(1) atoms with the oxygen atoms of the bridging ^{i}PrO groups in the Li_2O_2 planes. Additionally, four μ_2-^{i}PrO groups bridge the Li atoms and the external Ti atoms. Every Ti atom also has a terminal ^{i}PrO ligand. Thus, there are four distinct ^{i}PrO environments: four μ_3-^{i}PrO groups bridging two Li's and a Ti, four μ_2-^{i}PrO groups bridging one Li and one Ti, two terminal ^{i}PrO groups on internal Ti atoms, and two terminal ^{i}PrO groups on external Ti atoms. The four O^{2-} ions adopt μ_2- and μ_5-structural roles.

While there are two crystallographically-distinct Li environments, the coordination spheres of each are nearly identical. Each lithium is four-coordinate, but in a very unusual geometry in which Li lies below the base of a trigonal pyramid, with bonding to one μ_2-^{i}PrO, two μ_3-^{i}PrO, and one μ_5-O, which is at the apex. The internal Ti atoms have roughly octahedral coordination, with small deviations from linearity in O(7)–Ti(1)–O(15), and O(3)–Ti(1)–O(3)′ angles due to the fact that the $Ti(1)_2O(3)_2$ central

Table II. Fractional Coordinates[a] and Isotropic Thermal Parameters[b] for $[LiTiO(O^iPr)_3]_4$

	x	y	z	$10B_{iso}$, Å^2		x	y	z	$10B_{iso}$, Å^2
Ti(1)	2742.6(3)	6969.1(4)	761.2(4)	13	H(7)	73(2)	590(3)	213(3)	36(11)
Ti(2)	2234.5(3)	5802.8(4)	-430.5(4)	14	H(8)	403(3)	772(3)	202(3)	45(12)
O(3)	2674(1)	8048(1)	440(1)	13	H(9)	360(3)	666(3)	329(3)	48(14)
O(4)	2576(1)	5935(1)	624(1)	16	H(10)	429(3)	654(3)	266(3)	41(13)
Li(5)	3706(3)	8012(4)	-34(4)	19	H(11)	425(2)	711(3)	331(3)	29(11)
Li(6)	1693(3)	8173(3)	983(4)	19	H(12)	347(3)	828(3)	319(3)	43(12)
O(7)	1723(1)	7114(1)	1180(1)	15	H(13)	291(3)	829(3)	248(3)	30(11)
C(8)	1455(2)	6741(2)	1912(2)	21	H(14)	283(3)	775(3)	313(4)	56(17)
C(9)	1106(3)	7309(3)	2493(3)	29	H(15)	449(2)	686(2)	100(2)	8(7)
C(10)	927(3)	6141(3)	1656(3)	34	H(16)	389(2)	568(2)	101(3)	33(10)
O(11)	3165(1)	7037(1)	1790(1)	16	H(17)	422(3)	555(3)	6(3)	39(12)
C(12)	3603(2)	7428(2)	2368(3)	26	H(18)	475(2)	561(2)	80(3)	29(10)
C(13)	3981(3)	6885(3)	2938(3)	32	H(19)	543(2)	664(2)	5(3)	26(10)
C(14)	3167(3)	8000(3)	2830(3)	33	H(20)	489(2)	661(2)	-67(3)	29(11)
O(15)	3715(1)	6951(1)	170(1)	15	H(21)	506(2)	733(3)	-22(3)	31(11)
C(16)	4382(2)	6627(2)	466(2)	19	H(22)	190(2)	421(2)	62(2)	13(7)
C(17)	4311(2)	5795(3)	596(3)	28	H(23)	302(2)	358(2)	62(3)	24(10)
C(18)	4978(2)	6817(3)	-151(3)	25	H(24)	325(3)	387(3)	-20(4)	48(14)
O(19)	2129(1)	4796(1)	-419(2)	20	H(25)	316(2)	440(2)	61(2)	14(8)
C(20)	2178(2)	4136(2)	71(2)	21	H(26)	135(3)	360(2)	-58(3)	30(11)
C(21)	2958(3)	3994(3)	302(3)	30	H(27)	210(2)	340(2)	-93(3)	26(10)
C(22)	1840(3)	3497(3)	-406(4)	32	H(28)	187(3)	307(3)	-10(3)	50(15)
O(23)	1230(1)	6053(1)	-544(1)	16	H(29)	60(2)	525(2)	-39(2)	9(8)
C(24)	620(2)	5604(2)	-753(3)	22	H(30)	-13(2)	624(3)	-19(3)	30(12)
C(25)	-53(2)	6070(3)	-706(4)	30	H(31)	-4(2)	645(2)	-109(3)	24(10)
C(26)	710(3)	5258(4)	-1607(4)	43	H(32)	-50(3)	577(2)	-84(3)	32(10)
O(27)	2960(1)	5852(1)	-1285(1)	17	H(33)	27(3)	496(3)	-173(3)	40(12)
C(28)	3279(2)	5250(2)	-1758(2)	21	H(34)	73(2)	567(3)	-202(3)	33(13)
C(29)	3992(3)	5494(3)	-2119(4)	36	H(35)	113(3)	493(3)	-163(3)	41(12)
C(30)	2767(3)	4991(3)	-2439(3)	31	H(36)	339(2)	486(2)	-139(2)	10(8)
H(1)	185(2)	651(2)	222(2)	20(9)	H(37)	421(2)	509(3)	-240(3)	36(12)
H(2)	144(3)	770(3)	266(3)	39(13)	H(38)	391(3)	591(3)	-254(3)	40(13)
H(3)	68(2)	755(2)	223(3)	23(9)	H(39)	427(3)	568(3)	-172(3)	32(12)
H(4)	91(2)	708(2)	297(3)	28(10)	H(40)	228(3)	482(3)	-220(3)	50(13)
H(5)	53(3)	635(3)	137(3)	34(12)	H(41)	267(2)	537(3)	-281(3)	27(11)
H(6)	116(2)	582(2)	130(3)	22(10)	H(42)	299(2)	456(3)	-273(3)	33(11)

[a] Fractional coordinates are $\times 10^4$ for non-hydrogen atoms and $\times 10^3$ for hydrogen atoms. [b] Isotropic values for those atoms refined anisotropically are calculated using the formula given by W. C. Hamilton: Hamilton, W. C. *Acta Crystallogr.* **1959**, *12*, 609.

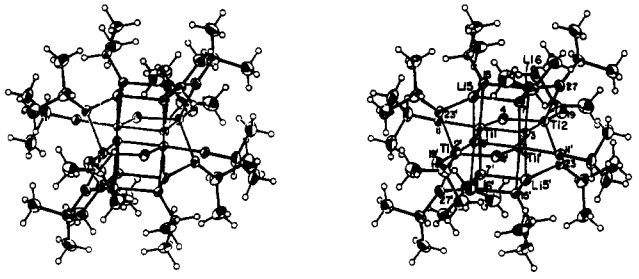

Figure 1. Stereo ORTEP drawing of $[LiTiO(O^iPr)_3]_4$, showing selected atom labeling.

rectangle is larger than either Li_2O_2 rectangle. These Ti atoms are coordinated by one terminal ^{i}PrO, two μ_3-^{i}PrO, one μ_2-O, and two μ_5-O's. The usual trend in bond distances is observed: terminal Ti–O^{i}Pr (1.8079(23) Å) < μ_3-Ti–O^{i}Pr (2.0145(22), 2.0262(22) Å), and μ_2-Ti–O (1.9164(23), 1.8899(24) Å) < μ_5-Ti–O (2.0013(22), 2.0499(23) Å). The wing Ti's have distorted trigonal bipyramidal coordination with O(3) and O(19) in the axial positions. The Ti atom sits on the O(19) side of the O(4)–O(23)–O(27) plane. Titanium(2) is coordinated to one μ_5-O, one μ_2-O, one terminal O^{i}Pr, and two μ_2-^{i}PrO. Again, the observed bond length trend is terminal Ti–O^{i}Pr (1.8132(25) Å) < μ_2-Ti–O^{i}Pr (1.9164(23), 1.9076(24) Å), and μ_2-Ti–O (1.7990(23) Å) < μ_5-Ti–O (2.0647(23) Å).

Solution Structure of $[LiTiO(O^iPr)_3]_4$. The NMR results support the contention that the molecule retains its solid-state structure in toluene solution and that there is no rapid alkoxide site exchange. The only implied fluxionality is a "flapping motion" of the exo $TiO(O^iPr)^+$ moieties to generate a time-averaged mirror plane relating the upper and lower halves of the two cubes. This plane passes through all four terminal isopropoxide ligands on Ti atoms, making the methyl environments of these equivalent by symmetry on the NMR time scale. As mentioned earlier, there are four different ^{i}PrO environments, with a 2:2:1:1 ratio; therefore, one expects four septets in the methine region with integrals of 2:2:1:1. All eight bridging ^{i}PrO groups have diastereotopic methyl groups, so the methyl region should be a set of six equal intensity doublets: 12 H's from terminal ^{i}PrO's on exterior Ti's, two diastereotopic sets of 12 from μ_2-^{i}PrO's, and two diastereotopic sets of 12 from μ_3-^{i}PrO's. This is exactly what is observed. Similarly, four methine and six methyl resonances are observed in the $^{13}C\{^1H\}$ NMR spectrum.

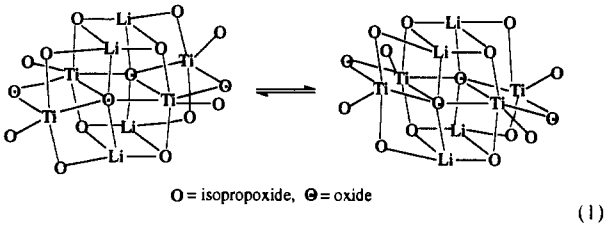

O = isopropoxide, Θ = oxide

(1)

In the temperature range -75 to +101 °C, only these peaks are observed, and no coalescence occurs. That is, on the NMR time scale, the "flapping motion" is not frozen out at -75 °C, and there is no ligand exchange at 101 °C. It is interesting to contrast this to the variable-temperature behavior of the precursor to this compound, $[LiTi(O^iPr)_5]_2$, where a coalescence temperature of 0 °C is observed. In $[LiTi(O^iPr)_5]_2$, Ti is pentacoordinate, which leaves one site open at each metal to form an alkoxide bridge and facilitate alkoxide migration. The internal Ti's in $[LiTiO(O^iPr)_3]_4$ are six-coordinate, which leaves no site open. Also, the oxo groups introduce a rigidity into the structure, which disfavors

Table III. Selected Bond Distances (Å) and Angles (deg) for $[LiTiO(O^iPr)_3]_4$

Ti(1)–O(3)	2.0013(22)	O(7)–C(8)	1.427(4)
Ti(1)–O(3)′	2.0499(23)	O(7)–Li(5)	1.991(6)
Ti(1)–O(4)	1.8899(24)	O(7)–Li(6)	1.922(6)
Ti(1)–O(7)	2.0145(22)	O(11)–C(12)	1.407(4)
Ti(1)–O(11)	1.8079(23)	O(15)–C(16)	1.438(4)
Ti(1)–O(15)′	2.0262(22)	O(15)–Li(5)	1.927(7)
Ti(2)–O(3)	2.0647(23)	O(15)–Li(6)	1.985(7)
Ti(2)–O(4)	1.7990(23)	O(19)–C(20)	1.416(4)
Ti(2)–O(19)	1.8132(25)	O(23)–C(24)	1.421(4)
Ti(2)–O(23)	1.9164(23)	O(23)–Li(5)	1.913(7)
Ti(2)–O(27)	1.9076(24)	O(27)–C(28)	1.439(4)
O(3)–Li(5)	2.050(6)	O(27)–Li(6)′	1.920(6)
O(3)′–Li(6)	2.019(6)		
O(3)–Ti(1)–O(3)′	75.82(10)	Ti(2)–O(3)–Li(5)	87.31(20)
O(3)–Ti(1)–O(4)	79.52(10)	Ti(2)–O(3)–Li(6)′	88.05(19)
O(3)′–Ti(1)–O(4)	155.01(10)	Li(5)–O(3)–Li(6)′	174.04(27)
O(3)–Ti(1)–O(7)	87.59(9)	Ti(1)–O(4)–Ti(2)	106.98(12)
O(3)′–Ti(1)–O(7)	84.32(9)	Ti(1)–O(7)–C(8)	122.19(21)
O(3)–Ti(1)–O(11)	175.35(10)	Ti(1)–O(7)–Li(5)	93.18(19)
O(3)′–Ti(1)–O(11)	101.01(10)	Ti(1)–O(7)–Li(6)	95.72(21)
O(3)–Ti(1)–O(15)	84.42(9)	Li(5)–O(7)–Li(6)	87.24(28)
O(3)–Ti(1)–O(15)′	87.34(9)	Ti(1)–O(11)–C(12)	149.99(24)
O(4)–Ti(1)–O(7)	90.68(10)	Ti(1)–O(15)′–C(16)′	127.89(21)
O(4)–Ti(1)–O(11)	103.85(10)	Ti(1)′–O(15)–Li(5)	93.13(20)
O(4)–Ti(1)–O(15)′	94.32(9)	Ti(1)′–O(15)–Li(6)	95.25(20)
O(7)–Ti(1)–O(11)	95.53(10)	Li(5)–O(15)–Li(6)	87.27(26)
O(7)–Ti(1)–O(15)′	169.64(9)	Ti(2)–O(19)–C(20)	145.90(23)
O(11)–Ti(1)–O(15)′	92.08(10)	Ti(2)–O(23)–C(24)	130.96(23)
O(3)–Ti(2)–O(4)	81.21(10)	Ti(2)–O(23)–Li(5)	95.77(20)
O(3)–Ti(2)–O(19)	178.52(10)	C(24)–O(23)–Li(5)	130.9(3)
O(3)–Ti(2)–O(23)	81.12(10)	Ti(2)–O(27)–C(28)	128.54(22)
O(3)–Ti(2)–O(27)	83.77(10)	Ti(2)–O(27)–Li(6)	95.72(21)
O(4)–Ti(2)–O(19)	99.14(11)	C(28)–O(27)–Li(6)	132.4(3)
O(4)–Ti(2)–O(23)	113.19(11)	O(3)–Li(5)–O(7)	88.22(24)
O(4)–Ti(2)–O(27)	113.99(11)	O(3)–Li(5)–O(15)	88.69(26)
O(19)–Ti(2)–O(23)	97.43(11)	O(3)–Li(5)–O(23)	81.59(25)
O(19)–Ti(2)–O(27)	97.37(11)	O(7)–Li(5)–O(15)	92.6(3)
O(23)–Ti(2)–O(27)	127.14(11)	O(7)–Li(5)–O(23)	124.0(3)
Ti(1)–O(3)–Ti(1)′	104.18(10)	O(15)–Li(5)–O(23)	141.5(3)
Ti(1)–O(3)–Ti(2)	92.22(9)	O(3)–Li(6)–O(7)	86.28(25)
Ti(1)–O(3)′–Ti(2)′	163.44(13)	O(3)–Li(6)–O(15)	86.30(26)
Ti(1)–O(3)–Li(5)	90.25(20)	O(3)–Li(6)–O(27)	84.70(25)
Ti(1)–O(3)′–Li(5)	90.43(19)	O(7)–Li(6)–O(15)	92.9(3)
Ti(1)–O(3)–Li(6)′	93.49(19)	O(7)–Li(6)–O(27)	147.9(4)
Ti(1)′–O(3)–Li(6)′	93.13(19)	O(15)–Li(6)–O(27)	117.1(3)

this site exchange. In addition, in $[LiTi(O^iPr)_5]_2$, all 10 ligands are capable of site exchange, whereas in $[LiTiO(O^iPr)_3]_4$, only 12 out of 16 ligands may migrate. All of these factors lead to slowed site exchange in the oxoalkoxide.

Synthesis of $BaZr_4(OH)(O^iPr)_{17}$. The hydrolysis of $BaZr_4(O^iPr)_{18}$ with 1 equiv of water proceeds in THF at room temperature with replacement of a μ_3-isopropoxide with a μ_3-hydroxide in a simple acid/base reaction. Tetrahydrofuran was chosen as solvent because both the precursor and water are soluble in it, allowing for slow delivery of the water by dropwise addition of wet THF. Since the hydroxide product is also water-sensitive, slow addition of water to precursor is important. The product also crystallizes nicely from THF providing a convenient "one-pot" synthesis.

Solid-State Structure of $BaZr_4(OH)(O^iPr)_{17}$. The structure (Figure 2) of $BaZr_4(OH)(O^iPr)_{17}$ consists of two face-shared, bioctahedral $Zr_2X_9^-$ units each bound to Ba^{2+} by four X groups. The groups X which bridge to barium are two terminal and two μ_2-X groups of each $X_3Zr(\mu_2\text{-}X)_3ZrX_3^-$ unit. One of the groups bridging to barium is the hydroxide.

Bond lengths from Zr to OR increase in the order Zr–O(terminal) (1.906(8)–1.945(16) Å) < Zr-μ_2–OBa (2.035(7)–2.068(7) Å) < Zr–μ_2-OZr (2.190(7)–2.211(7) Å) < Zr–μ_3-O^iPr (2.245(6)–2.256(6) Å). Distances from zirconium to the μ_3-OH group (2.198(7) and 2.259(6) Å) are quite comparable to those to the μ_3-O^iPr groups. While Ba–μ_2-OR distances fall in quite a narrow range (2.782(7)–2.794(7) Å), the Ba–μ_3-O^iPr distances are quite variable (2.790(6)–3.076(7) Å). The distance to the μ_3-OH group is much shorter (2.660(6) Å). Consistent with this irregularity of the barium coordination sphere, the O–Ba–O bond angles fail to conform to either of the standard eight-particle polyhedra, or even to any molecular symmetry element. Zr–O(terminal)–C angles (163.6(6)–178.4(7)°) approach linearity. Coordination at the oxygen atoms of the Zr_2O^iPr groups is planar, and nearly so at the $BaZrO^iPr$ groups (angles sum to 355.9–360.0°).

An examination of the infrared spectrum indicates the absence of any hydrogen bonding[11] for the OH group, in spite of its expected high Bronsted acidity. There are no significantly long Zr–O^iPr distances (which would suggest that such a group was actually coordinated ^iPrOH); this supports our assignment of the μ_3-ligand (O(6)) as hydroxide, not oxide.

Solution Structure and Dynamics of $BaZr_4(OH)(O^iPr)_{17}$. The $^{13}C\{^1H\}$ NMR spectrum of $BaZr_4(OH)(O^iPr)_{17}$ at −32 °C in toluene-d_8 shows, in the methyl region, many resonances which are generally overlapped and poorly resolved. The methine carbons are slightly more informative and show 10 distinct resonances of unequal intensity, whereas 17 are expected for the structure determined in the solid state. The remainder of the resonances must therefore either be accidentally equivalent or equilibrated by some fluxional process.

The ^1H NMR spectra at +86 and at +107 °C in toluene-d_8 show only two unequal intensity methyl doublets consistent with a 9:8 population of O^iPr groups. Accordingly, the methine proton region shows two overlapping septets. We interpret this as indicating migration (site exchange) of all O^iPr groups *within* their original $BaZr_2$ triangle, but no migration onto the second $BaZr_2$ triangle. The hydroxyl group differentiates the two $BaZr_2$ groups, and must also *not* migrate to the second $BaZr_2$ group at 107 °C in order to satisfy the observed spectra. The doublet which integrates to eight (and therefore corresponds to the ^iPrO groups on the *hydroxyl* $BaZr_2$ triangle) is much broader than the other doublet. Thus, introduction of the hydroxide slows the fluxional process, much like the oxide did for $[LiTiO(O^iPr)_3]_4$ as compared to $[LiTi(O^iPr)_5]_2$. As the temperature is lowered, the two methyl doublets broaden, then resolve into more doublets. At 25 °C, the spectral pattern is poorly resolved due to slower site exchange and an increased number of resonances. At −12 and −32 °C, line widths are again sharper, but by −52 °C, they appear broad again, presumably as the expected 2 × 17 methyl environments cease to be time-averaged. Variable-temperature spectra are available as Supplementary Material. The entirety of the variable-temperature NMR results are consistent with retention of the solid-state molecular structure in toluene even at +107 °C.

Discussion

The balanced hydrolysis reaction for $[LiTi(O^iPr)_5]_2$ (eq 2) proceeds with retention of the 1:1 ratio of lithium and titanium.

$$2[LiTi(O^iPr)_5]_2 + 4H_2O \rightarrow [LiTiO(O^iPr)_3]_4 + 8\,^iPrOH \quad (2)$$

Although alcohol is released in the reaction, it does not coordinate to any metal in the product. The degree of aggregation grows, as a result of this partial hydrolysis, from two to four. This is because oxide has greater bridging capacity (e.g., μ_5) than alkoxide, together with the incipient *reduction* in ligand-to-metal ratio as *two* alkoxide ions are replaced by *one* O^{2-}. If alcohol had remained coordinated, a dimeric form, $[LiTiO(O^iPr)_3(^iPrOH)_2]_2$,

(11) The shortest observed O/O distances are from O6 to O43 and O51 (terminal alkoxides), and these are neither bent at O nor far from their metal, as they would be if hydrogen bonding were present. See: Vaartstra, B. A.; Huffman, J. C.; Gradeff, P. S.; Hubert-Pfalzgraf, L. G.; Daran, J.-C.; Parraud, S.; Yunlu, K.; Caulton, K. G. *Inorg. Chem.* **1990**, *29*, 3126.

Table IV. Fractional Coordinates and Isotropic Thermal Parameters[a] for $BaZr_4(OH)(O^iPr)_{17}$

	10^4x	10^4y	10^4z	$10B_{iso}$, Å^2		10^4x	10^4y	10^4z	$10B_{iso}$, Å^2
Ba(1)	1263.1(1)	6799(1)	677.7(3)	21	C(38)	1301(2)	4443(12)	-445(7)	51
Zr(2)	676.1(2)	6360(1)	1355(1)	26	O(39)	2050(1)	6687(6)	1658(3)	25
Zr(3)	709.0(2)	8270(1)	196(1)	27	C(40)	2277(2)	6494(9)	1973(6)	33
Zr(4)	1802.4(2)	8014(1)	1569.9(5)	23	C(41)	2450(2)	6687(12)	1436(7)	48
Zr(5)	1835.1(2)	5494(1)	1097.6(5)	22	C(42)	2320(2)	7169(11)	2612(6)	42
O(6)	908(1)	7748(5)	1193(3)	23	O(43)	676(1)	6743(6)	2330(3)	32
O(7)	753(1)	6532(5)	231(3)	26	C(44)	709(2)	7009(11)	3027(6)	48
C(8)	688(2)	5725(9)	-279(6)	37	C(45)	492(3)	6844(12)	3364(7)	58
C(9)	799(2)	5966(11)	-951(6)	42	C(46)	806(3)	8101(13)	3116(8)	69
C(10)	434(2)	5666(12)	-415(6)	53	O(47)	449(1)	5250(7)	1322(4)	42
O(11)	1609(1)	6490(5)	1726(3)	20	C(48)	264(4)	4593(16)	1457(11)	108
C(12)	1523(2)	6098(9)	2375(5)	29	C(49)	176(4)	3930(20)	1044(12)	129
C(13)	1335(2)	6838(9)	2592(5)	30	C(50)	321(5)	4129(28)	2201(17)	208
C(14)	1712(2)	5985(10)	2951(5)	35	O(51)	703(1)	9694(6)	537(4)	35
O(15)	1757(1)	7069(5)	583(3)	24	C(52)	701(2)	10767(11)	773(6)	45
C(16)	1813(2)	7506(9)	-74(5)	33	C(53)	626(2)	10812(11)	1506(7)	53
C(17)	1678(2)	6928(10)	-660(5)	40	C(54)	558(3)	11428(12)	277(8)	68
C(18)	2069(2)	7466(10)	-162(6)	37	O(55)	504(1)	8382(7)	-633(4)	38
O(19)	971(1)	5474(6)	1365(4)	29	C(56)	329(2)	8559(12)	-1166(6)	50
C(20)	1046(2)	4458(9)	1613(6)	35	C(57)	180(4)	9448(21)	-998(9)	122
C(21)	1006(2)	4319(10)	2361(6)	38	C(58)	417(3)	8725(21)	-1805(8)	111
C(22)	937(2)	3556(10)	1178(7)	47	O(59)	1819(1)	8490(5)	2531(3)	26
O(23)	1026(1)	8236(6)	-206(3)	30	C(60)	1880(2)	8932(10)	3193(5)	41
C(24)	1154(2)	8877(10)	-656(6)	38	C(61)	1996(3)	9959(13)	3136(8)	70
C(25)	1079(2)	10004(11)	-671(7)	47	C(62)	1677(3)	9021(14)	3612(6)	61
C(26)	1133(2)	8358(13)	-1378(7)	57	O(63)	2004(1)	9059(6)	1207(4)	34
O(27)	461(1)	7635(6)	892(3)	30	C(64)	2146(3)	9922(14)	1080(8)	77
C(28)	245(2)	8118(11)	1002(6)	40	C(65)	2097(2)	10390(10)	372(7)	51
C(29)	202(3)	8170(15)	1756(7)	66	C(66)	2356(3)	9914(17)	1399(8)	89
C(30)	60(2)	7486(16)	600(8)	73	O(67)	1859(1)	4354(6)	1769(4)	32
O(31)	1489(1)	8589(5)	1238(3)	27	C(68)	1874(3)	3338(12)	2105(8)	58
C(32)	1358(2)	9535(9)	1214(6)	33	C(69)	1648(3)	2988(12)	2300(7)	58
C(33)	1489(2)	10429(10)	898(7)	51	C(70)	2058(2)	3309(12)	2648(7)	51
C(34)	1293(2)	9859(10)	1944(6)	45	O(71)	2057(1)	4953(5)	488(3)	27
O(35)	1541(1)	5029(5)	536(3)	26	C(72)	2239(2)	4398(9)	216(5)	31
C(36)	1513(2)	4255(10)	11(6)	48	C(73)	2154(2)	3765(11)	-421(7)	49
C(37)	1527(3)	3164(12)	288(7)	60	C(74)	2354(2)	3722(11)	773(7)	46

[a] Isotropic values for those atoms refined anisotropically are calculated using the formula given by Hamilton: Hamilton, W. C. *Acta Crystallogr.* **1959**, *12*, 609.

could have all Ti centers six-coordinate. It is this enhanced aggregation, then, which frustrates coordination of the alcohol released in eq 2. Finally, it is noteworthy that the tetrameric product *lacks* 4-fold symmetry, giving rise to inequivalent titanium environments. The five-coordinate titanium atoms in $[LiTiO(O^iPr)_3]_4$ presumably could provide growth sites for additional aggregation in further hydrolysis.

The double cube core structure reported here has some similarity to the structure reported[12] recently for $Li_5Sm(O^tBu)_8$. The four equivalent lithiums in II adopt the same geometry as

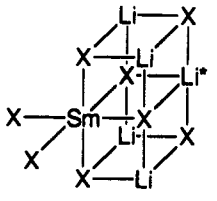

X = O^{t}Bu

II

found in $[LiTiO(O^iPr)_3]_4$, while Li* in II adopts the distorted lithium coordination geometry found in $[LiTi(O^iPr)_5]_2$. Such structures represent efficient ways of approaching the preferred coordination numbers of the metals involved, as the molecular structure simultaneously evolves toward that of a pure oxide solid. The core of the $[LiTiO(O^iPr)_3]_4$ structure begins to resemble the cubic perovskite oxide lattice of known ferroelectric titanates. In the cubic perovskite, as in $[LiTiO(O^iPr)_3]_4$, the Ti atoms are in a central plane of the lattice, surrounded by oxygen atoms. One can also see the early stages of formation of metal–oxygen layers in this compound. Such layers are thought to be important in determining electrical properties in ferroelectric and superconducting materials.[13] The alkoxide R groups terminate the oxy-ligand functionality at a maximum of μ_3, and thus halt growth at a molecular, rather than infinite lattice, situation.

The structures of $BaZr_4X(O^iPr)_{17}$ are very similar for X = O^{i}Pr[7] and X = OH. The X-ray study shows that the hydroxide is in a triply bridging site. We propose that this is a thermodynamic preference: the μ_3-O^{i}Pr group is quite an unlikely *kinetic* site of hydrolysis since such a group lacks a lone pair for attack by a water proton.[14] Given the variety of alternative sites for the hydroxyl group, the thermodynamic bias for μ_3-OH must be considerable. However, the ^{i}PrO moiety would be predicted to adopt the more bridging position based upon relative basicity of the oxygen centers involved ($pK_a^{H_2O}$ = 15.7, pK_a^{iPrOH} = 18).[15] Therefore, the controlling factor in this case must be a *steric* preference for OH^- to adopt a μ_3 position.

Although the two $BaZr_4X(O^iPr)_{17}$ species have very similar molecular structures, they are *not* crystallographically isomorphous. Moreover, while the two $BaZr_2$ triangles have a dihedral angle of 37° when X = O^{i}Pr, this angle is 66° when X = OH. The solubility of $BaZr_4(O^iPr)_{17}(OH)$ in THF is dramatically lower than that of its precursor. Presumably, this is a result of decreased hydrophobic character in the ligand set. Furthermore,

(12) Schumann, H.; Kociok-Köhn, Dietrich, A.; Görlitz, F. *Z. Naturforsch* **1991**, *46B*, 896.

(13) Cava, R. J. *Science* **1990**, *247*, 656. Simon, A.; Mattansch, H.; Eger, R.; Kremer, R. K. *Angew. Chem., Int. Ed. Engl.* **1991**, *30*, 1188.

(14) Based on the demonstrated fluxionality of the molecule in solution, the reaction is almost certainly under thermodynamic control.

(15) Lowry, T. H.; Richardson, K. S. *Mechanism and Theory in Organic Chemistry*; Harper and Row: New York, 1987; p 300.

Table V. Selected Distances (Å) and Angles (deg) for $BaZr_4(OH)(O^iPr)_{17}$

Ba(1)–Zr(2)	3.816(1)	Zr(2)–O(47)	1.925(8)	Ba(1)–O(19)	2.794(7)	Zr(4)–O(39)	2.211(7)
Ba(1)–Zr(3)	3.798(1)	Zr(3)–O(6)	2.275(7)	Ba(1)–O(23)	2.787(7)	Zr(4)–O(59)	1.945(6)
Ba(1)–Zr(4)	3.813(1)	Zr(3)–O(7)	2.198(7)	Ba(1)–O(31)	2.790(7)	Zr(4)–O(63)	1.933(7)
Ba(1)–Zr(5)	3.773(1)	Zr(3)–O(23)	2.068(7)	Ba(1)–O(35)	2.782(7)	Zr(5)–O(11)	2.245(6)
Zr(2)–Zr(3)	3.296(2)	Zr(3)–O(27)	2.204(7)	Zr(2)–O(6)	2.247(7)	Zr(5)–O(15)	2.246(7)
Zr(4)–Zr(5)	3.302(1)	Zr(3)–O(51)	1.906(8)	Zr(2)–O(7)	2.259(6)	Zr(5)–O(35)	2.058(7)
Ba(1)–O(6)	2.660(6)	Zr(3)–O(55)	1.939(7)	Zr(2)–O(19)	2.057(7)	Zr(5)–O(39)	2.195(7)
Ba(1)–O(7)	3.076(7)	Zr(4)–O(11)	2.256(6)	Zr(2)–O(27)	2.190(7)	Zr(5)–O(67)	1.930(7)
Ba(1)–O(11)	2.790(6)	Zr(4)–O(15)	2.245(6)	Zr(2)–O(43)	1.944(6)	Zr(5)–O(71)	1.941(6)
Ba(1)–O(15)	2.939(7)	Zr(4)–O(31)	2.035(7)				

Zr(2)–Ba(1)–Zr(3)	51.30(5)	O(15)–Zr(4)–O(59)	165.27(26)	O(6)–Zr(2)–O(27)	73.36(26)	Zr(4)–O(11)–C(12)	127.3(6)
Zr(4)–Ba(1)–Zr(5)	51.60(5)	O(15)–Zr(4)–O(63)	95.11(27)	O(6)–Zr(2)–O(43)	89.17(27)	Zr(5)–O(11)–C(12)	121.8(6)
Ba(1)–Zr(2)–Zr(3)	64.07(4)	O(31)–Zr(4)–O(39)	150.08(26)	O(6)–Zr(2)–O(47)	168.9(3)	Ba(1)–O(15)–Zr(4)	93.73(20)
Ba(1)–Zr(3)–Zr(2)	64.62(4)	O(31)–Zr(4)–O(59)	100.0(3)	O(7)–Zr(2)–O(19)	80.44(26)	Ba(1)–O(15)–Zr(5)	92.40(21)
Ba(1)–Zr(4)–Zr(5)	63.57(4)	O(31)–Zr(4)–O(63)	102.0(3)	O(7)–Zr(2)–O(27)	71.80(24)	Ba(1)–O(15)–C(16)	112.8(6)
Ba(1)–Zr(5)–Zr(4)	64.82(4)	O(39)–Zr(4)–O(59)	99.84(26)	O(7)–Zr(2)–O(43)	157.1(3)	Zr(4)–O(15)–Zr(5)	94.66(22)
O(6)–Ba(1)–O(7)	51.58(19)	O(39)–Zr(4)–O(63)	97.0(3)	O(7)–Zr(2)–O(47)	102.9(3)	Zr(4)–O(15)–C(16)	121.7(6)
O(6)–Ba(1)–O(11)	109.88(18)	O(59)–Zr(4)–O(63)	98.5(3)	O(19)–Zr(2)–O(27)	149.30(25)	Zr(5)–O(15)–C(16)	132.2(6)
O(6)–Ba(1)–O(15)	140.96(19)	O(11)–Zr(5)–O(15)	68.83(22)	O(19)–Zr(2)–O(43)	100.7(3)	Ba(1)–O(19)–Zr(2)	102.68(27)
O(6)–Ba(1)–O(19)	64.07(20)	O(11)–Zr(5)–O(35)	86.31(24)	O(19)–Zr(2)–O(47)	100.9(3)	Ba(1)–O(19)–C(20)	120.4(6)
O(6)–Ba(1)–O(23)	64.41(19)	O(11)–Zr(5)–O(39)	72.25(23)	O(27)–Zr(2)–O(43)	100.0(3)	Zr(2)–O(19)–C(20)	136.9(6)
O(6)–Ba(1)–O(31)	81.86(20)	O(11)–Zr(5)–O(67)	93.81(26)	O(27)–Zr(2)–O(47)	97.9(3)	Ba(1)–O(23)–Zr(3)	101.93(25)
O(6)–Ba(1)–O(35)	151.24(19)	O(11)–Zr(5)–O(71)	166.60(26)	O(43)–Zr(2)–O(47)	99.3(3)	Ba(1)–O(23)–C(24)	118.2(6)
O(7)–Ba(1)–O(11)	146.26(17)	O(15)–Zr(5)–O(35)	83.07(26)	O(6)–Zr(3)–O(7)	68.67(24)	Zr(3)–O(23)–C(24)	137.8(7)
O(7)–Ba(1)–O(15)	160.20(16)	O(15)–Zr(5)–O(39)	73.11(24)	O(6)–Zr(3)–O(23)	83.84(24)	Zr(2)–O(27)–Zr(3)	97.19(25)
O(7)–Ba(1)–O(19)	56.54(19)	O(15)–Zr(5)–O(67)	162.40(26)	O(6)–Zr(3)–O(27)	72.57(24)	Zr(2)–O(27)–C(28)	137.6(6)
O(7)–Ba(1)–O(23)	57.66(19)	O(15)–Zr(5)–O(71)	99.42(25)	O(6)–Zr(3)–O(51)	89.9(3)	Zr(3)–O(27)–C(28)	124.6(7)
O(7)–Ba(1)–O(31)	128.59(19)	O(35)–Zr(5)–O(39)	152.33(26)	O(6)–Zr(3)–O(55)	166.0(3)	Ba(1)–O(31)–Zr(4)	103.31(26)
O(7)–Ba(1)–O(35)	116.84(19)	O(35)–Zr(5)–O(67)	99.3(3)	O(7)–Zr(3)–O(23)	83.36(27)	Ba(1)–O(31)–C(32)	114.7(6)
O(11)–Ba(1)–O(15)	52.52(17)	O(35)–Zr(5)–O(71)	98.96(28)	O(7)–Zr(3)–O(27)	72.72(25)	Zr(4)–O(31)–C(32)	141.9(7)
O(11)–Ba(1)–O(19)	90.70(19)	O(39)–Zr(5)–O(67)	99.4(3)	O(7)–Zr(3)–O(51)	157.7(3)	Ba(1)–O(35)–Zr(5)	101.40(24)
O(11)–Ba(1)–O(23)	147.16(20)	O(39)–Zr(5)–O(71)	98.64(27)	O(7)–Zr(3)–O(55)	99.3(3)	Ba(1)–O(35)–C(36)	125.8(7)
O(11)–Ba(1)–O(31)	61.89(19)	O(67)–Zr(5)–O(71)	97.4(3)	O(23)–Zr(3)–O(27)	151.07(27)	Zr(5)–O(35)–C(36)	128.7(7)
O(11)–Ba(1)–O(35)	63.86(18)	Ba(1)–O(6)–Zr(2)	101.75(25)	O(23)–Zr(3)–O(51)	100.9(3)	Zr(4)–O(39)–Zr(5)	97.09(25)
O(15)–Ba(1)–O(19)	137.85(19)	Ba(1)–O(6)–Zr(3)	100.35(22)	O(23)–Zr(3)–O(55)	102.30(28)	Zr(4)–O(39)–C(40)	137.9(6)
O(15)–Ba(1)–O(23)	109.83(19)	Zr(2)–O(6)–Zr(3)	93.60(25)	O(27)–Zr(3)–O(51)	95.7(3)	Zr(5)–O(39)–C(40)	125.0(6)
O(15)–Ba(1)–O(31)	59.12(19)	Ba(1)–O(7)–Zr(2)	89.98(21)	O(27)–Zr(3)–O(55)	97.5(3)	Zr(2)–O(43)–C(44)	171.9(8)
O(15)–Ba(1)–O(35)	59.85(19)	Ba(1)–O(7)–Zr(3)	90.57(22)	O(51)–Zr(3)–O(55)	101.1(3)	Zr(2)–O(47)–C(48)	164.1(10)
O(19)–Ba(1)–O(23)	112.29(21)	Ba(1)–O(7)–C(8)	118.1(6)	O(11)–Zr(4)–O(15)	68.65(22)	Zr(3)–O(51)–C(52)	178.4(7)
O(19)–Ba(1)–O(31)	125.96(20)	Zr(2)–O(7)–Zr(3)	95.36(24)	O(11)–Zr(4)–O(31)	83.74(25)	Zr(3)–O(55)–C(56)	170.3(8)
O(19)–Ba(1)–O(35)	87.48(20)	Zr(2)–O(7)–C(8)	121.8(6)	O(11)–Zr(4)–O(39)	71.74(24)	Zr(4)–O(59)–C(60)	166.9(7)
O(23)–Ba(1)–O(31)	85.36(21)	Zr(3)–O(7)–C(8)	130.5(6)	O(11)–Zr(4)–O(59)	97.08(25)	Zr(4)–O(63)–C(64)	167.8(10)
O(23)–Ba(1)–O(35)	136.68(19)	Ba(1)–O(11)–Zr(4)	97.60(22)	O(11)–Zr(4)–O(63)	162.16(27)	Zr(5)–O(67)–C(68)	164.8(8)
O(31)–Ba(1)–O(35)	114.56(19)	Ba(1)–O(11)–Zr(5)	96.47(20)	O(15)–Zr(4)–O(31)	82.58(26)	Zr(5)–O(71)–C(72)	163.6(6)
O(6)–Zr(2)–O(7)	68.12(23)	Ba(1)–O(11)–C(12)	112.9(5)	O(15)–Zr(4)–O(39)	72.81(24)		
O(6)–Zr(2)–O(19)	84.45(25)	Zr(4)–O(11)–Zr(5)	94.36(22)				

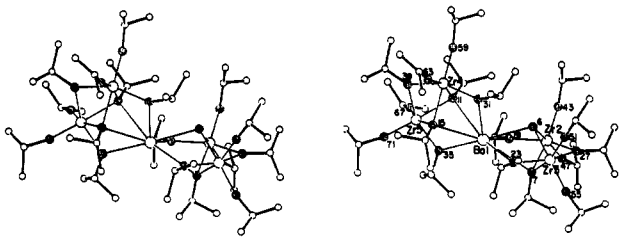

Figure 2. Stereo ORTEP drawing of the nonhydrogen atoms of $BaZr_4(OH)(O^iPr)_{17}$, showing selected atom labeling. Stippled atoms are oxygen; small open circles are carbon.

OH^- slows ligand site exchange relative to the all-$^iPrO^-$ precursor. Even without any aggregation, partial hydrolysis has introduced some rigidity to the molecule's framework. Changing one ligand in the set also serendipitously makes it possible to establish that all site exchange is local to a $BaZr_2$ triangle, without migration of hydroxide to the second $BaZr_2$ triangle in the molecule. This is probably also the case for $BaZr_4(O^iPr)_{18}$ but the symmetry of that molecule masks NMR detection.

A question of some interest is why the isopropoxide migration is local to a $BaZr_2$ triangle, and not global (i.e., over the entire $BaZr_4$ molecular framework). Such a global intramolecular migration would require a transition state in which alkoxide is terminal on barium. Moreover, it is probable that the lowest energy process would involve concerted migration of one alkoxide from each triangle into such terminal positions (see eq 3). We

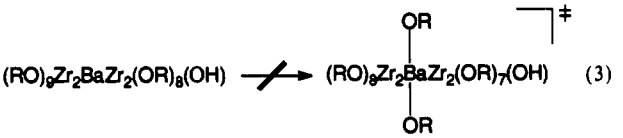

suggest that it is not inherently unfavorable to have alkoxide terminal on barium, but instead the loss of donor ligands on Zr(IV) is the factor making this a high-energy process. The high Lewis acidity and oxophilicity of Zr(IV), and its propensity for a coordination number of six, make "surrender" of a bridging alkoxide entirely to barium energetically costly. In summary, although the molecule is fluxional, concerted (pairwise) migration between terminal, μ_2 and μ_3 sites is best accomplished only within one $BaZr_2$ triangle.

Conclusions

We report here two hydrolysis intermediates of homoleptic mixed-metal alkoxides. The metal stoichiometry of each is retained during hydrolysis, which is an encouraging result for the molecular precursor approach. The molecules characterized here provide some understanding of the early stages of hydrolysis of a heterometallic alkoxide:

(1) The $BaZr_4(OH)(O^iPr)_{17}$ example is the simplest in that it shows no increase in aggregation. Because of the preference of

the hydroxide for a μ_3 site and as a result of the steric protection of that site by its many neighboring ^{i}Pr groups, the acidic OH proton is not accessible to further aggregation to a second $BaZr_4$ unit. One can predict from this result that a considerable degree of hydrolysis (e.g., > $4H_2O/BaZr_4$ unit) will be required before aggregation (through $BaZr(\mu_2\text{-OH})$ or $Zr_2(\mu_2\text{-OH})$ functionality) will begin.

(2) In contrast to the above case, where all zirconium centers are six-coordinate, $[LiTi(O^iPr)_5]_2$ has only five-coordinate titanium. This, together with the general preference of Ti(IV) to be six-coordinate, is crucial to the fact that this molecule aggregates ($Li_2Ti_2 \rightarrow Li_4Ti_4$) on hydrolysis. Note, however, that the degree of hydrolysis is larger for $Li_2Ti_2(O^iPr)_{10}$ ($2H_2O$/mol) than it is for $BaZr_4(O^iPr)_{18}$ (one H_2O/mol). The ratio of H_2O per O^iPr group differs even more dramatically.

Acknowledgment. This material is based upon work supported under a National Science Foundation Graduate Fellowship, the U.S. Army, (Contract DASG 60-92-C0025), and the Department of Energy. We thank John A. Samuels for thoughtful insights into these results.

Supplementary Material Available: Tables giving full crystallographic details and anisotropic thermal parameters, a fully labelled drawing for each compound, and variable-temperature ^{1}H NMR spectra for $BaZr_4(OH)(O^iPr)_{17}$ (8 pages). Ordering information is given on any current masthead page.